ADAPTIVE MESH NUMERICAL SOLUTION OF THE ELECTRO-MAGNETIC FLOWMETER FOR PARTIALLY- FILLED PIPES

Prof. Saleh Esmael Najem   Dr. Qais A. Rashak   Mr. Muneer A. Ismael
University of Basrah- Colleague of Engineering- Mechanical Eng. Department

Abstract:

Electromagnetic flowmeters measure flow rate of the electrically conducting liquids. Its operation is based on Faraday's principle of induction. In many situations the pipe may be partially filled where in this case the analysis of the flowmeter equation is widely altered and the numerical solution may diverge.

In this paper we have established a new numerical formulation, based on finite difference method, which adaptively refines the mesh until the desired solution converges to a certain accuracy.

The representation of the flowmeter equations in the polar axis of the solution domain (cylindrical cut from it the empty portion) can result in the singularities in the solution. To avoid these singularities, the grids are shifted one half mesh width from the polar axis.

The number of iterations that gives convergence is appreciably reduced via this numerical technique. The build algorithm of the adaptive numerical solution led us to determine, for each liquid level, the optimum angular position of the electrodes that gives maximum accuracy i.e. minimum sensitivity to the changes in the velocity profile of the liquid to be metered.

<div dir="rtl">

حل عددي متكيف الشبكة لمقياس الجريان الكهرمغناطيسي في حالة أنبوب ممتلئ جزئيا

أ.د. صالح اسماعيل نجم   د. قيس عبد الحسن رشك   السيد منير عبد الجليل اسماعيل
جامعة البصرة ـ كلية الهندسة ـ قسم الهندسة الميكانيكية

الخلاصة:

إن مقياس الجريان الكهرومغناطيسي الذي يعمل وفق مبدأ الحث الكهرومغناطيسي لفرداي يقيس معدل التدفق للسوائل الموصله كهربائيا. أحيانا يكون الأنبوب ممتلىء جزئيا بالسائل المراد قياس معدل جريانه ففي هذه الحالة يتغير الحل النظري و ربما يتباعد الحل العددي.

في هذه الدراسة أسسنا طريقة عددية جديدة، أعتمادا على طريقة الفروقات المحددة، حيث يمكن تنعيم شبكة الحل في مناطق معينة حتى نصل إلى الحل الصحيح و بالدقة المطلوبة.

قد تظهر أثناء الحل نقاط إنفرادية (singularities) نتيجة للشكل الهندسي لمجال الحل لذلك فقد ظهرت عندنا نقاط إنفرادية واقعة على محور المقياس (flowmeter axis) ولتجنب هذه النقاط تم تزحيف شبكة الحل بأكملها عن هذا المركز بمقدار نصف المسافة بين عقدتين متجاورتين بالأتجاه القطري.

بفضل هذه الطريقة الجديدة لوحظ أن هنالك تناقص في عدد التكرارات التي تحقق التقارب في الحل العددي. إن البرنامج الذي تم تطويره يقوم بمجرد إعطائه مستوى السائل في الأنبوب بأيجاد الموقع الأمثل للاقطاب اشارة الجريان المحتثة و الذي بدوره يقلل من تأثر مقياس الجريان الكهرومغناطيسي بالتغيرات الحاصلة في منحنى السرعة.

</div>

List of Symbols

A	Cross-sectional area of the flow
B	Magnetic flux density vector
d_{min}	Mesh ill-conditioning criterion
e_{crit}	Critical error criterion
e_{max}	Max. error
$e_{min.}$	Min. error
F	Magnetic scalar
G	Virtual current scalar
J_v	Virtual current density vector
i,j,k	Node notations of the initial coarse mesh
n	Normal vector
r,θ,z	Cylindrical coordinates
R_o	Inner radius of the flowmeter
v	Liquid velocity vector
W	Weight vector
W_z	Axially integrated weight function
$\overline{W}_z$	Average of W_z
ΔU	Flowmeter signal
$\Delta r, \Delta \theta, \Delta z$	Intervals of the initial coarse finite difference mesh
β,γ	Selectable factors
ε	Weight function non-uniformity measure
θe	Angular position of electrode
τ	Flowmeter measuring volume

Introduction

Electromagnetic Flowmeter (EMF) measures flow rate of electrically conducting liquids, its operation is based on Faraday's principle of induction; a magnetic field is applied across the pipe, the moving liquid is considered as a homogenous conductor and the induced voltage in the liquid is proportional to its velocity. This induced voltage is picked up by two electrodes positioned in the non magnetic and non conducting pipe of the flowmeter (liner), see figure1. The performance of the
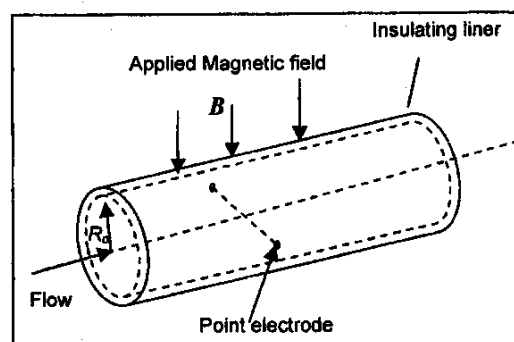

Fig.1. Principle of the electromagnetic flowmeter

EMF is determined by the magnetic field, which is determined by the magnetic coil geometry, and the virtual current field, which in turn is determined by the shape, position and number of the electrodes.

More-high level mathematics has probably been applied to the EMF than any other flowmeters. Shercliff [1] discussed the general theory of this device. Bevir in 1970 [2] has given an elegant analysis of the device using the concept of the weight function that connects the magnetic field and the virtual current field. However, the weight function concept is widely used in studying the extending of compatibility between the flowmeter design and the flow patterns. However, most of the reported studies and the available EMF are designed

where the measuring section is fully-filled with liquid. The literature survey has shown that there is a very little published works relating the measurement of a partially-filled flow using the EMF. Knowing that the partially- filled flow frequently occurs in the waste water lines of large industrial plants, or with rain retention reservoirs. Zhang in 1998 [3] introduced the first theoretical analysis regarding the distribution of the virtual current field through the partially filled flowmeter. He developed an alternating analysis method but in two dimensions.

In the present study we intend to analyze the partially-filled EMF in an alternating numerical method. Our numerical method is based on finite difference scheme which refines the mesh automatically i.e. adaptive mesh refining. This means that the computational efforts are concentrated in the regions where the error is higher than a predetermined limit. This adaptive solution helps in earlier convergence with less storage capacity also it should provide greater flexibility when applied to situations complicated by flow profiles, pipe geometry and different electrode positions. The numerical process is achieved in three- dimensional, cylindrical coordinates to solve Laplace's equations for the magnetic and the virtual current fields.

Basic Theory of the Electromagnetic Flowmeter

The basic equation of the EMF has been derived by Shercliff [1];

$$\nabla^2 U = \nabla.(v \times B) \qquad \ldots (1)$$

Where U is the electric potential in the liquid, v is the liquid velocity vector and B is the magnetic flux density. In the low liquid conductivity application, rather than the liquid metal, the most general solution of the equation above is given by [2];

$$\Delta U = \int_\tau W.v\,d\tau \qquad \ldots (2)$$

Where τ is flowmeter volume occupied by liquid and W is the weight vector, the powerful concept that developed by Bevir. Bevir introduced W as [2];

$$W = B \times J_v \qquad \ldots (3)$$

Where J_v is the current density that would exist in the flow tube in the absence of the magnetic field and flow if unit current enters by one electrode and extracted by the other, He termed it as the virtual current. J_v describes completely the boundary conditions of the flow channel and electrode geometry. Generally the distribution of W gives the response of the EMF, for a given flow rate, to the variations in the velocity distribution. The most common used criterion measure of the non-uniformity distribution of the weight function is ε, where;

$$\varepsilon = \frac{1}{A} \int_A \left| 1 - \frac{W_z}{\overline{W_z}} \right| r\,dr\,d\theta \qquad \ldots (4)$$

Where

$$W_z = \int_{-\infty}^{+\infty} W(r,\theta,z)\,dz$$

$$\overline{W_z} = \frac{1}{A} \int_A W_z\, r\, dr\, d\theta$$

A is the area of pipes that is wetted by liquid.

The distribution of B and Jv result from a scalar potential function F an G respectively which are governed by Laplace equation as shown below [4];

$$B = \nabla F$$

$$\nabla^2 F = 0 \qquad \ldots (5)$$

And

$$J_v = \nabla G$$

$$\nabla^2 G = 0 \qquad \ldots (6)$$

Where Laplace's operator in 3D cylindrical coordinates is;

$$\nabla^2 = \frac{\partial^2}{\partial r^2} + \frac{1}{r}\frac{\partial}{\partial r} + \frac{1}{r^2}\frac{\partial^2}{\partial \theta^2} + \frac{\partial^2}{\partial z^2}$$

Where r,θ,z are the cylindrical coordinates. Solving F and G with their own boundary conditions, the distribution of B and J_v and hence W can be obtained.

What was introduced above is the general theory of all types of EMF and what follows here is the numerical treatment of the partially-filled EMF.

Numerical Formulation of the Irregular Difference Approximations

In a partially-filled flowmeter we lose the symmetry over the horizontal axis hence, we need to solve J_v for one-fourth of the flowmeter volume. We decided to use the finite difference method but with automatically increasing the resolution of the mesh grids in the high error regions or as is often said *adaptive solution*. The reasons that led us to establish such solutions are: firstly, the liquid level inside the flowmeter is variable therefore the size and shape of the virtual current domain is variable also and secondly, the position of the pick up electrodes is no longer diametrically opposite, as in the conventional EMFs, their position may be angularly shifted. Both the two reasons above may lead to the absence of the solution convergence.

Laplace's equation of the virtual current scalar potential G in 3-D Cylindrical coordinates is:

$$\nabla^2 G = \frac{\partial^2 G}{\partial r^2} + \frac{1}{r}\frac{\partial G}{\partial r} + \frac{1}{r^2}\frac{\partial^2 G}{\partial \theta^2} + \frac{\partial^2 G}{\partial z^2}$$

Each term of the equation above was approximated using Taylor's series basing on irregular intervals as follows;

$$\frac{\partial G}{\partial r} = \frac{G(i+1,j,k) - G(i-1,j,k)}{\Delta r_1 + \Delta r_2}$$

$$\frac{\partial^2 G}{\partial r^2} = \frac{2}{\Delta r_1 + \Delta r_2 \Delta r_1} G(i+1,j,k) + \frac{2}{\Delta r_2 + \Delta r_1 \Delta r_2} G(i-1,j,k)$$

$$\frac{\partial^2 G}{\partial \theta^2} = \frac{2}{\Delta\theta_1 + \Delta\theta_2 \Delta\theta_1} G(i, j+1, k) +$$

$$\frac{2}{\Delta\theta_2 + \Delta\theta_1 \Delta\theta_2} G(i, j-1, k)$$

$$\frac{\partial^2 G}{\partial z^2} = \frac{2}{\Delta z_1 + \Delta z_2 \Delta z_1} G(i, j, k+1) +$$

$$\frac{2}{\Delta z_2 + \Delta z_1 \Delta z_2} G(i, j, k-1)$$

Where i, j, k represent node points along radial, azimuthal, and axial directions respectively, $\Delta r_{1,2}$, $\Delta\theta_{1,2}$ and $\Delta z_{1,2}$ represent the radial, azimuthal and axial intervals respectively. From the programming simplicity point of view the ordering of the potential G is transformed from $G(i,j,k)$ to $G(i)$ only i.e. contracting the three dimensional array of G to only one dimensional array. This procedure was developed by Emad [5]. In this new ordering, $(i+1,j,k)$ becomes no(i) (where no- north) and $(i-1,j,k)$ becomes so(i) (so-south). Also Δr_1 becomes S_1 and Δr_2 becomes S_2 and so on for the other coordinates (see fig. 2). Accordingly, we need additional matrices, six of them for denoting the six neighboring nodes and three for the node localization definition due to r, θ and z coordinates. Here i does not mean radial node point, its value is i=1,2,3,4....N where N is the total number of the initial mesh nodes in the domain. This new ordering helps in giving a clear imaging for the

refinement process Referring to notations of figure 2, the virtual current scalar G can be written as;

$$G_i = St * \begin{bmatrix} \left(\frac{1}{Sn(Sn+Ss)} + \frac{1}{2r(Sn+Ss)}\right)G(no(i)) + \\ \left(\frac{1}{Ss(Sn+Ss)} - \frac{1}{2r(Sn+Ss)}\right)G(so(i)) + \\ \frac{1}{r^2}\left(\frac{1}{Sw(Sw+Se)}\right)G(we(i)) + \\ \frac{1}{r^2}\left(\frac{1}{Se(Sw+Se)}\right)G(es(i)) + \\ \frac{1}{Sf(Sf+Sb)}G(fr(i)) + \\ \frac{1}{Sb(Sf+Sb)}G(ba(i)) \end{bmatrix} \quad ..(7)$$

Where

$$\frac{1}{St} = \frac{1}{Sn(Sn+Ss)} + \frac{1}{Ss(Sn+Ss)} + \frac{1}{r^2}\left[\frac{1}{Se(Se+Sw)} + \frac{1}{Sw(Se+Sw)}\right] + \frac{1}{Sf(Sf+Sb)} + \frac{1}{Sb(Sf+Sb)}$$

The solution of the magnetic field, **B,** is also subjected to the adaptive procedure. The irregular differences equation of the magnetic scalar F is as same as that of equation (7) with replacing each G by F. Note that the magnetic permeability of the metered liquid (say water) and the air existing in the empty portion of the flowmeter are the

38

same, hence, the magnetic field distribution is not affected by the liquid level inside the flowmeter.
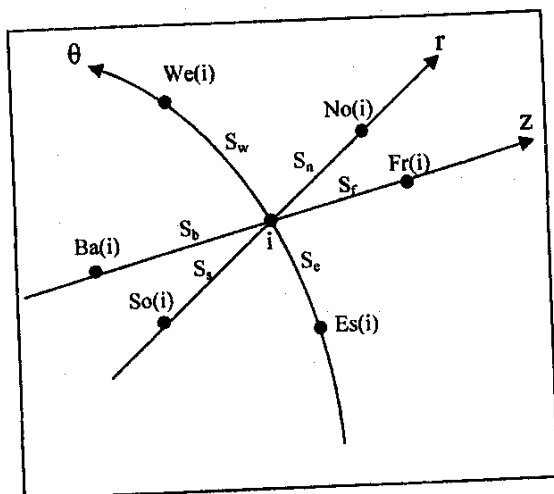

Fig.2. 3-D, Cylindrical coordinates Notations of the numerical solution

Adaptive Procedure

Additional nodes are added in the interest regions is the concept of the h-adaptive method which is modified in this study to be compatible with cylindrical coordinates and liquid level variations. The procedure of the adaptive method is as follows:

1-An initial, uniform, coarse mesh is generated. Then this initial mesh is stored as one dimensional array to simplify the refinement process. For each node in the

initial uniform mesh, we fix its local coordinates r, θ, and z and the six neighboring nodes; North (No) and South (So) in the r direction; East (Es) and West (We) in θ direction and Front (Fr) and Back (Ba) in z direction as shown in figure 2.

2- The approximation error of each node is calculated and among all nodes we determine the maximum and minimum errors.

3-After a specified iteration, if the percentage approximation error of any node exceeds the predetermined (critical) error, this node is marked to be source of adding three new nodes, one in each direction. The position of each new added node is halfway the distance between the marked node and its neighboring one.

4- After any adding or (refining) process, the mesh must be updated due to change in the neighboring nodes.

5- The obtained new mesh which is composed of the initial and newly added nodes is resolved and then repeating step 2.

6- The adding process is continued until the error in each node becomes under or equal the critical error.

The critical error (or as is often said, the *error criterion*) is given by [6]:

$$e_{crit} = e_{max} - \beta(e_{max} - e_{min}) \qquad \dots (9)$$

Where:

e_{crit}: is the critical error or the minimum node error required to be marked for refinement.

e_{max}: is the maximum node error in the mesh.

e_{min}: is the minimum node error in the mesh

β: selectable factor, $0<\beta<1$.

In order to avoid an ill-conditioned mesh, the distance between the newly added node and any other node in the domain is limited to being greater than or equal to a minimum predetermined distance [7]. This minimum distance may be considered as another criterion of the refining process as:

$$d_{min} = \gamma * d_{max}$$

Where d_{max} represents the interval of the initial uniform mesh and as follows;

In radial direction $d_{max}= \Delta r$, in azimuthal direction $d_{max}= \Delta\theta$, and axially $d_{max}= \Delta z$ and $0< \gamma <1$

The boundary conditions of the partially-filled EMF can be summarized as follows (figure 3.):

1- F=constant on the pipe area occupying the two magnetic pole pieces (+1 for upper coil and -1 for the lower coil). This is due to the high magnetic permeability of the magnet yoke.

2-The optimum boundary condition of F was developed by [4] which are:

$F=f(\theta)$ and $F=-f(\theta)$, where f is a function results from the numerical optimization of

F. For further details, the interest can refer to ref [4]

3- G=constant on the electrode

4- G=0 on the two ends of the flowmeter

5- $\dfrac{\partial G}{\partial n} = 0$ on the;

(a) Liquid free surface

(b)Insulating flow tube excepting the electrodes.

Where n is a normal vector.

What remains is that the refining or adding algorithm must distinguish the nodes that cause a divergent refinement series. In the cylindrical geometry of our interest, these nodes (geometric singularities) exist on the polar axis (flowmeter centerline) and they are excluded by shifting all the mesh grids one-half grid in the radial direction [8], hence;

$$A_r = \frac{2R_o}{2(N_r - 1)+1}$$

$$r_i = \left(i - \frac{1}{2}\right)A_r$$

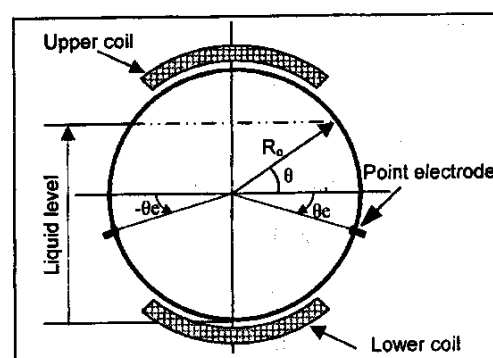Fig. 3 partially-filled cross-sectional pipe

Where Δ_r is the radial interval and N_r is the number of nodes in the r-direction. Both Δ_r and N_r refer to the initial coarse mesh before adding.

Results and Discussions

Using the above mentioned boundary conditions, in this study we fixed the magnetic field boundary condition to be of an optimum type [4], while the pick up electrodes was a single pair of point type. It is quite clear from equ.(9) that for larger β values the number of flagged nodes to be adapted will increases and vice versa. For different positions of point electrodes, the number of iterations against different values of β is shown in figure 4. The implication that could be observed from this figure is that increasing the added nodes (higher β values) is no longer leads to faster convergence (less iteration). The reason of this may be attributed to the truncation, residual or approximation errors accompanying to the excessively increased nodes. Another show could be extracted from the same figure, that is, for the same liquid level, the number of total nodes required for the best convergence is larger when the electrode position tends to be farther (larger θe) from the liquid free surface. The reason of this, we believe, may be the following; the high error in the solution is generated mainly due to the existing of the liquid free surface where

there is no virtual current flow across it and due to the electrode itself, hence, when the electrode position is narrow from the free surface, the number of nodes required will be limited meanwhile on the other hand, the solution requires say individually added nodes to the high error regions when the electrodes move away from the liquid free surface. Figure 5 indicates that the solution of the magnetic scalar potential F has no demand to the adapting the mesh, this was expected for two reasons. Firstly, the magnetic field B does not affected by the partially filled flow case, and secondly, the boundary conditions of F were already determined by an optimization procedure. Altogether, it is clear that the best value of β that gives faster convergence is 0.2-0.3 for the virtual current solution and 0.0 for the magnetic field solution.

The value of γ, the constant of the ill-conditioning mesh criterion, was fixed at 0.25 in all numerical calculations; this was obtained after many experiment runs.
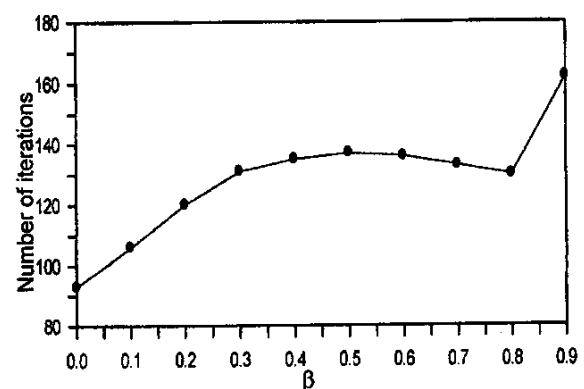

Fig. 5 Effect of β on the number of iterations of solving magnetic scalar F.

To ensure that the convergence is going toward the correct solutions; the distribution of nodes through the flowmeter volume were examined using the scatter graphs of Mat lab software; these graphs, figure 6-9, which were presented for liquid level of 1.6 R_o, imply that the nodes are more dense near the electrode position and this means that the refinement process is concentrated, as expected, near the high error regions. Figure 10 also shows the distribution of the nodes of the magnetic field scheme.
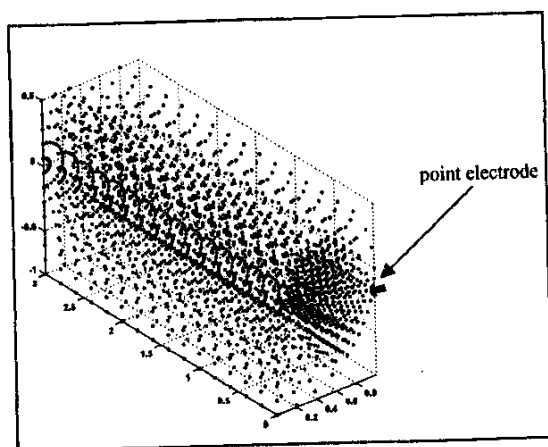

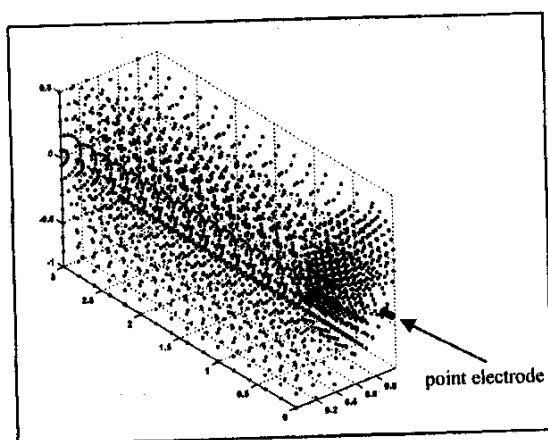Fig. 6 Nodes distribution of G mesh, $\theta_e=0°$, $\beta=0.2$. Total number of nodes is 2640

Fig. 7 Nodes distribution of G mesh, $\theta_e=22°$, $\beta=0.2$. Total number of nodes is 2793

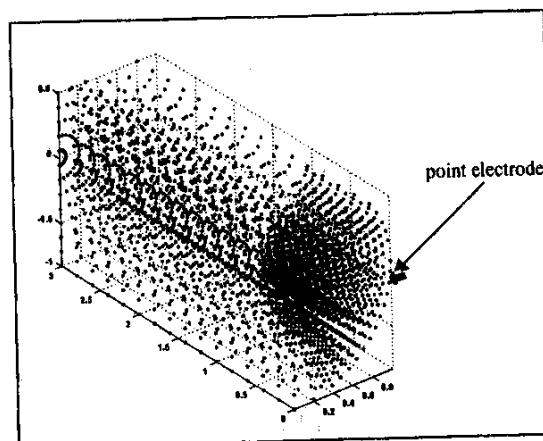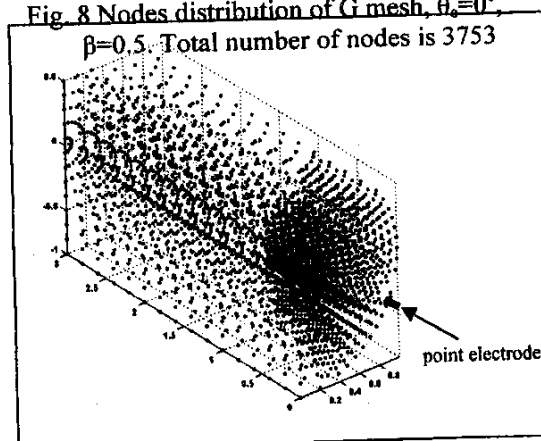Fig. 8 Nodes distribution of G mesh, $\theta_e=0°$, $\beta=0.5$. Total number of nodes is 3753

Fig. 9 Nodes distribution of G mesh, $\theta_e=22°$, $\beta=0.5$. Total number of nodes is 3859
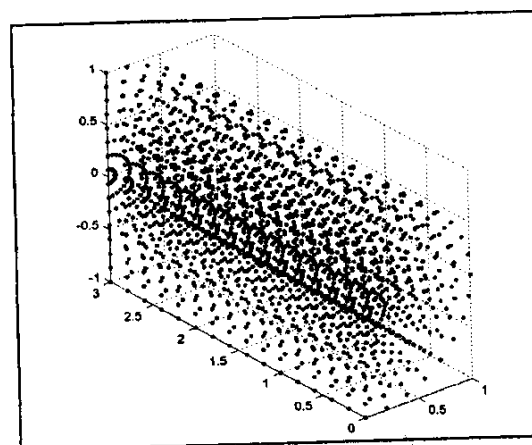

Fig.10 Nodes distribution of F mesh, optimum magnetic field

Figure 11 shows the variations of ε versus both the liquid level and the angular position of electrodes. From this figure we can extract the suitable angular position for each liquid level. Generally, when $\theta_e > 0$, increasing the liquid level lead to an increase in the ε, this relation is completely inverted when $\theta_e = 0$. Since the value of ε increases with electrode position, the best position of the electrode pair is 11° below the horizontal flowmeter axis.

stability. Mesh refining process was excited in a region if that region obeys two criteria, these are; the critical error which depends on the geometry of both the magnet and the electrodes together with a selectable factor β. The other criterion, d_{min}, serves in avoiding the mesh ill-conditioning. The 3D visualizations of the node clouds led us to confirm that the regimes of maximum error lay close to the liquid free surface and electrodes. Also these visualizations have showed that the polar singularities were safely avoided by the v ting the
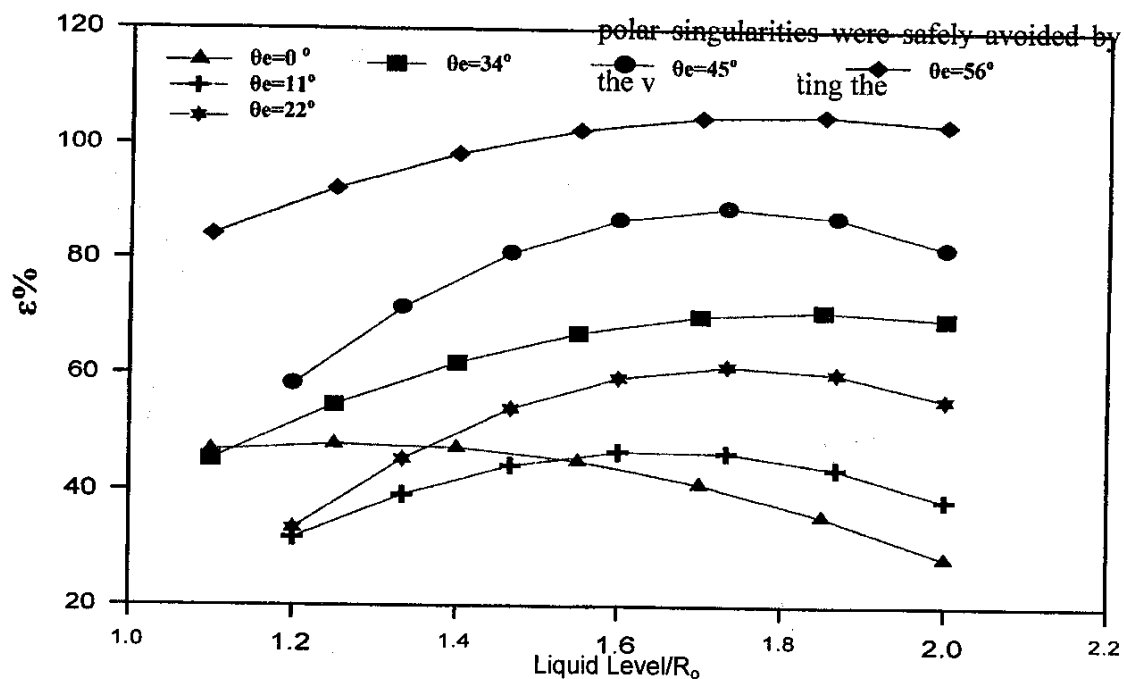

Fig. 11 Variation of ε with the electrode angular position and the liquid level

Conclusions

The flexible and reliable adaptive numerical method was established to treat the partially-filled electromagnetic flowmeter, where little literatures were found about this subject, with low storage capacity and appreciable convergence and mesh grids one-half radial grid ($0.5\Delta r$). The weight function non-uniformity measure ε and the electrode positions together with the liquid level were gathered in a revealing map. This

map told us that the optimum position of the single pair of commercially point electrodes is $\theta_e = 11^\circ - 22^\circ$, knowing that the applied magnetic field is of an optimum type.

The present adaptive algorithm has proved that it not only stabilizes and increases the accuracy of the finite difference solution, but it also helpful to overcome the poorness of the original mesh grids especially when the liquid level becomes much low. Henceforth, it is possible, using this promising adaptive technique, to deal with the application of the electromagnetic flowmeters for plenty flow patterns like two phase bubbly, slug, annular flows where the solution domain of the virtual current in these cases becomes more complicated and irregular.

Keeping in mind that this numerical technique could be used in fully-filled flow applications where the Neumann boundary condition on the free surface is removed in this case.

References

[1] J.A. Shercliff "The theory of electromagnetic flow-measurement" Cambridge: Cambridge university press. (1962)

[2] M.k.Bevir "The theory of induced voltage electromagnetic flowmeter" Journal of phys. E. Sci. Instrum. Vol.17, pp 577-590, (1970).

[3] X.Z. Zhang "The virtual current of an electromagnetic flowmeter in partially filled pipes" Measurement Sci. and Technol. Vol.9, pp 1852-1855 (1998).

[4] M.A. Ismael "Optimization, design and test of an electromagnetic flowmeter" MSc. Thesis, University of Basrah (1998).

[5] Emad A. Khazal "Adaptive finite difference solution of NSE in laminar incompressible 2D flow in a step channel" MSc Thesis, University of Basrah, 1999

[6] J.R. Tristano, Z. Chen, D.A. Hancq, W. Kowk "Fully automatic adaptive mesh refinement integrated into the solution process" ANSYS incorporated, Canonsburg, PA U.S.A.

[7] F. Urena, J.J. Benito, and R. Alvarez "Computational error approximation and h-adaptive algorithm for 3-D generalized finite difference method" International Journal for Computational Methods in Engineering Science and Mechanics. Vol. 6, pp 31,39 (2005).

[8] C.L. Ming, W.L. Wen and W. Weichung "A fast spectral/difference method without pole conditions for Poisson-type equations in cylindrical and spherical geometries" IMA Journal of Numerical analysis" vol. 22, pp 537-548 (2002).